ELSEVIER

Contents lists available at ScienceDirect

Anthropocene

journal homepage: www.elsevier.com/locate/ancene





Sensitivity of a meandering lowland river to intensive landscape management: Lateral migration rates before and after watershed-scale agricultural development

Bruce L. Rhoads ^{a,*}, Alison M. Anders ^b, Poushalee Banerjee ^c, David A. Grimley ^d, Andrew Stumpf ^d, Neal E. Blair ^e

- ^a Department of Geography and Geographic Information Science, University of Illinois at Urbana-Champaign, Urbana, IL 61801, USA
- b Department of Earth Science and Environmental Change, University of Illinois at Urbana-Champaign, Urbana, IL 61801, USA
- ^c Department of Geology and Environmental Science, University of Pittsburgh, Pittsburgh, PA 15260, USA
- d Illinois State Geological Survey, Praire Research Institute, University of Illinois, Champaign, IL 61820, USA
- ^e Department of Earth and Planetary Science, Northwestern University, Evanston, IL 60208, USA

ARTICLE INFO

Keywords: Agriculture Geomorphology Lateral migration Meandering river Radiocarbon dating

ABSTRACT

Agricultural development has transformed the vegetation cover of many landscapes around the world, thereby altering water and sediment fluxes to river systems. Past work in the upper midwestern United States, particularly in areas of moderate relief, has shown that increases in water and sediment fluxes associated with agricultural development have dramatically altered river dynamics. Less is known about how agriculture has affected river dynamics, particularly rates of lateral migration, in relatively low relief landscapes of the Midwest shaped by glaciation during the Wisconsin Episode. This research examines rates of lateral migration of a channel bend along a lowland meandering river in Illinois, USA before and after agricultural development. The rate of lateral migration prior to agricultural development is estimated through dating of carbonaceous material within lateralaccretion deposits underlying distinct meander scrolls. The rate of lateral migration after agricultural development is determined from analysis of changes in river-channel position determined from survey records, aerial imagery, and digital elevation data. Average rates of migration before and after agricultural development are similar, suggesting that agricultural development has not substantially affected rates of lateral migration of the river. Some accelerated movement occurred locally following agricultural development, but this movement cannot be definitively tied to landscape transformation. Possible factors responsible for the lack of sensitivity of the river system to agricultural development include high resistance of the cohesive, tree-lined riverbanks to erosion and the low bankfull stream power per unit area of the modern river. From a management perspective, the study highlights the importance of bank vegetation in maintaining channel stability in low-relief agricultural landscapes.

1. Introduction

Humans have become major agents of landscape change. Agriculture is a prominent human activity that has affected many landscapes; according to recent estimates, 48 % of habitable land globally is used for agriculture (Richie, 2019). In the United States, about 52 % of the total land area is dedicated to agriculture (Bigelow and Borchers, 2017) and in the upper Midwest, agricultural land use encompasses as much as 90 % of the total area of some watersheds (Kumar et al., 2018).

Transformation of landscapes from native vegetation to agriculture through land clearing and frequent tillage of soil associated with farming can radically change the delivery of water and sediment to river systems (Rhoads, 2020). Following European settlement in the 19th century, vast areas of the upper Midwest, originally covered by prairie and forest, were converted to agricultural land (Rhoads and Herricks, 1996; Anders et al., 2018; Wilson et al., 2018; Kumar et al., 2023). The effect of intensive agriculture practices on river systems in the loess-covered Driftless Area, a part of the upper Midwest that either was

E-mail addresses: brhoads@illinois.edu (B.L. Rhoads), amanders@illinois.edu (A.M. Anders), pob13@pitt.edu (P. Banerjee), dgrimley@illinois.edu (D.A. Grimley), astumpf@illinois.edu (A. Stumpf), n-blair@northwestern.edu (N.E. Blair).

^{*} Corresponding author.

not glaciated during the Pleistocene Epoch or lacks preservation of glacial deposits, has been extensively documented (Carson et al., 2019). Clearing of land increased runoff from hillslopes, resulting in enhanced flooding and high rates of soil erosion (Knox, 1977, 1987, 2001; Trimble, 2013). Sediment supplied to headwater portions of stream networks translated down these networks in wave-like fashion (Trimble, 2009, 2013). More frequent overbank flows transported sediment-laden waters onto floodplains, producing pronounced floodplain aggradation (Happ, 1944; Trimble, 1983; Magilligan, 1985; Knox, 1987; Beach, 1994; Lecce, 1997; Faulkner, 1998; Belby et al., 2019). Increases in the erosive power of streams and rivers caused by increases in flood magnitudes as well as by increases in channel depth related to floodplain aggradation led to channel enlargement and high rates of meander migration, especially in the headwaters and middle parts of watersheds (drainage areas of \sim 20–150 km²) (Knox, 1987, 2001; Lecce, 1997). Adjustment of rivers systems in the Driftless Area is ongoing, with rates and spatial patterns of adjustment influenced by implementation of soil conservation practices beginning in the 1940s (Trimble, 2013).

Less is known about river responses to watershed-scale human activity in relatively low-relief portions of the Midwest affected by the Wisconsin Episode, especially depositional landscapes shaped by retreat of the ice margin during late stages of this glacial period. Work to date has focused mainly on the fate of sediment eroded from farmed lowrelief uplands. Most of this eroded sediment is stored on hillslopes or in closed depressions, rather than on floodplains (Beach, 1994; Blair et al., 2022). Post-settlement rates of floodplain sedimentation are an order of magnitude greater than those prior to European settlement – a finding consistent with post-settlement floodplain sedimentation rates in other areas of the Midwest with relatively high relief (Grimley et al., 2017). On the other hand, the total thickness of post-settlement floodplain alluvium is much less than that documented in the Driftless Area (Magilligan, 1992; Knox, 2006) or similar landscapes of northeastern and southwestern Iowa (Baker, a, b et al., 1993) that were last glaciated prior to the Illinois Episode (Hallberg et al., 1984; Rovey and McLouth, 2015; Dalton et al., 2020). Studies of the response of headwater meandering streams in low-relief landscapes affected Wisconsin-Episode glaciation to human impact indicate that these fluvial systems respond slowly to channel straightening associated with channelization. Many headwater streams remain straight for several decades following channelization (Urban and Rhoads, 2003; Rhoads et al., 2016). Rates of increase in channel sinuosity for reaches that do exhibit recovery to straightening depend on stream power per unit area of bankfull flow, but full recovery of pre-channelized sinuosity for even the fastest recovering reaches is on the order of a century or more (Salas and Rhoads, 2022).

In contrast to these investigations of floodplain sedimentation and direct human impacts on river systems through channel modifications, few, if any, studies have examined how rates of lateral migration of unchannelized meandering rivers in low-relief glaciated landscapes of the Midwest have responded to implementation of agriculture at watershed scales. This type of analysis requires information on lateral migration rates prior to and following the advent of agriculture. The high rates of meander migration of some Driftless-Area streams due to human-induced increases in runoff and sediment delivery are consistent with studies of meandering river dynamics, which indicate that meander-migration rates depend directly on sediment supply (Constantine et al., 2014; Ahmed et al., 2019; Donovan et al., 2021), discharge (Hooke, 1980, 1987; Schook et al., 2017; Moody, 2022; Clavijo-Rivera et al., 2023), and stream power (Nanson and Hickin, 1983, 1986; Larsen et al., 2006; Güneralp and Rhoads, 2009). Thus, increases in runoff and sediment delivery related to agricultural land use should increase rates of lateral migration as the river system adjusts to accommodate these inputs (Quik et al., 2020). Although changes in land use have been associated with changes in the planform of meandering rivers (Morais et al., 2016), research on the impact of such changes on lateral migration is noticeably lacking (James and Lecce, 2013).

The purpose of this study is to explore the following research question: Is the current lateral migration rate of a lowland meandering river within an intensively managed watershed in the agricultural Midwest that was glaciated during the Wisconsin Episode similar to or different from the lateral migration rate prior to widespread human modification of land cover? The goal is to shed light on the sensitivity of river systems in recently glaciated environmental settings to human modification of landscape conditions at watershed scales. This type of information will provide insight into the extent to which intensive agriculture in these settings is affecting river dynamics - important knowledge that can be used to guide river and watershed management.

2. Study reach and watershed characteristics

The study reach is a 900 m long meander bend of the Sangamon River located in the Upper Sangamon River Basin in east-central Illinois (Fig. 1). The bend is located in the Allerton Park and Recreation Center, a 607-hectare property owned by the University of Illinois that is relatively undisturbed compared to the surrounding landscape. The floodplain within the park is covered by old growth and secondary old growth forest (Illinois Natural Areas Inventory, 2023). The river channel has a bankfull width of 30 m, is 3–4 m deep, and has a channel slope of 0.00026. Bed material consists mainly of sand and fine gravel. The bend was selected for analysis because its interior exhibits several distinct curvilinear features on high-resolution lidar images that become more pronounced in appearance near the river channel (Fig. 1). The features are interpreted as relict scrolls that demarcate lateral migration of the bed toward the position of its outer bank.

Upstream of the study reach the USRB has a drainage area of 1500 km². The Sangamon River basin was last glaciated during the Wisconsin Episode with ice covering the landscape about 20,000 to 24,000 years ago (Curry et al., 2011; Grimley et al., 2016). Prior to this most recent glaciation, the landscape was also glaciated during the Illinois Episode and by pre-Illinois ice advances (Anders et al., 2018). These repeated glaciations have deposited 50-150 m of unconsolidated sediment (Soller et al., 1999; Stumpf and Dey, 2012) consisting of layers of dense loamy till and glacial outwash along with some interbedded layers of glacio-lacustrine sediment (Kempton et al., 1991; Grimley et al., 2016). End moraines, including the Champaign and Cerro Gordo moraines, constitute local high areas that form drainage divides for the USRB (Illinois Department of Natural Resources, 1999; Grimley et al., 2016). The upper surface of the land is covered by 0.5-1.5 m of loess (Fehrenbacher et al., 1986). The dominant soil type is poorly to moderately drained Mollisols. Total relief in the watershed is 100 m and the median gradient of hillslopes is less than 1 %. The modern valley of the Sangamon River, which is about 550-600 m wide and bordered by river bluffs, likely was carved during retreat of the Lake Michigan Lobe of the southern Laurentide Ice Sheet (Grimley et al., 2016). Local relief between the uplands and the valley bottom is about 10 to 15 m.

Pre-settlement vegetation in the watershed was predominantly prairie (88 % of land cover) with scattered forest that occurred mainly within the riparian corridor of the Sangamon River (Illinois Department of Natural Resources, 1999). In the mid to late 1800 s most of the watershed was converted into agricultural land. Today nearly 90 % of the land is farmed (Rhoads et al., 2016). Major crops include corn and soybeans. Many headwater stream channels have been straightened and in other areas artificial channels have been added to the drainage network; as a result, drainage density has increased three-fold throughout the watershed (Rhoads et al., 2016). Floodplains in the USRB have a distinct layer of post-settlement alluvium about 0.5–0.9 m. thick (Grimley et al., 2017).

3. Data and methods

Evaluation of rates of lateral migration of the study bend prior to intensive agricultural development of the region focused on

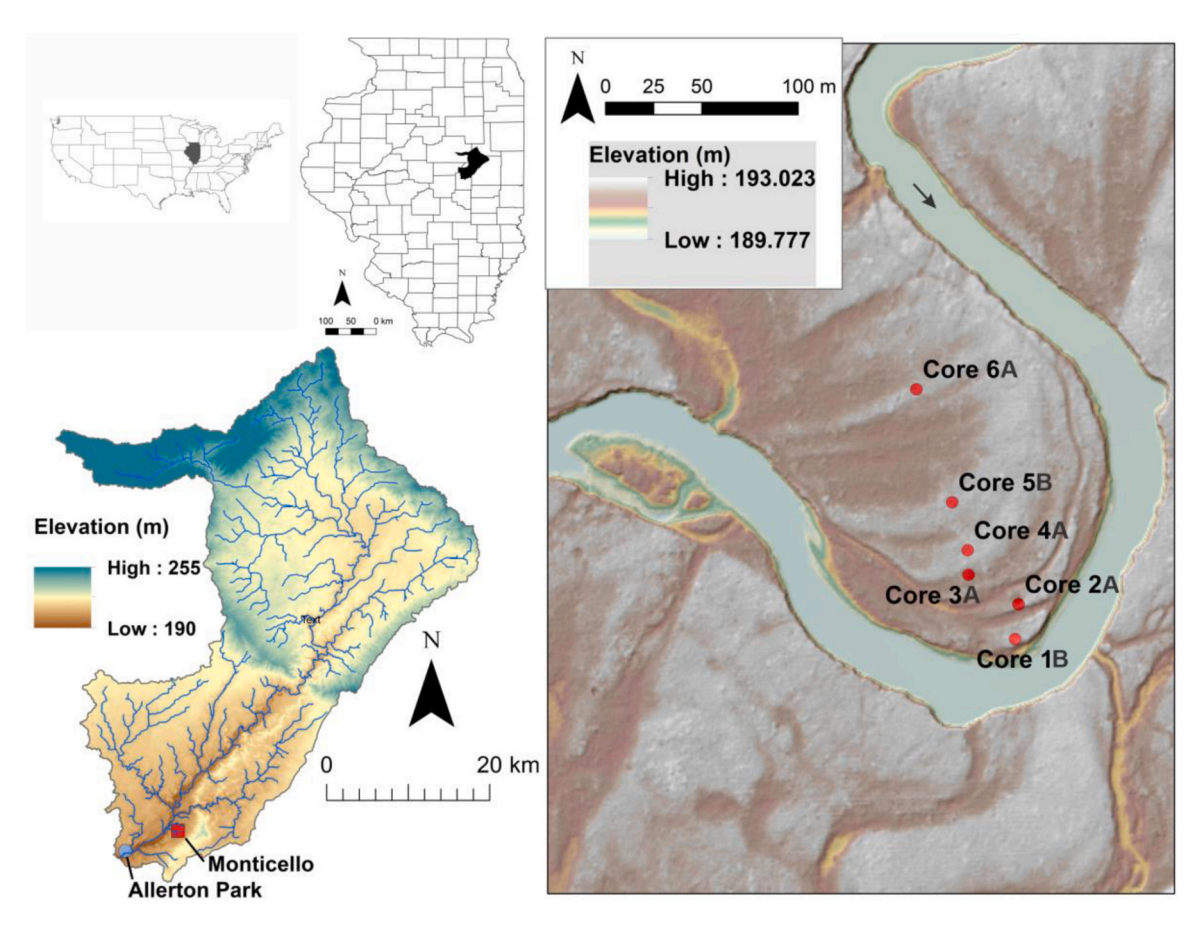


Fig. 1. Location of the Sangamon River basin within Illinois, USA (upper left), the Sangamon River basin upstream of Allerton Park (lower left), and the study bend and coring locations within Allerton Park (right). Remnant scroll bars are evident as topographic highs (gray tones) on the interior of the bend. Arrow indicates direction of river flow.

identification and dating of lateral-accretion deposits in cores of the floodplain sediment obtained from positions of distinct meander scrolls, which mark past inner bank positions of the river (Mason and Mohrig, 2019). If dateable carbonaceous material (wood, leaves, or shells) is contemporaneous with the lateral-accretion deposits sediment within which it is situated (i.e. it was not mobilized from long-term depositional storage and then redeposited), radiocarbon dating of this material will constrain the ages of scroll-bar formation. Differences in ages of lateral-accretion deposits corresponding to successive scroll bars will demarcate the time it took the meander bend to migrate over the distance between the scrolls. A similar approach based on dating of the exposure of sand grains in lateral-accretion deposits to light using optically stimulated luminescence has proven effective at determining long-term lateral migration rates of meander bends (Rodnight et al., 2005; Quik and Wallinga, 2018). It is also consistent with dating of scroll bar positions using dendrochronology (Schook, 2017; Liu et al., 2021). The position of the channel in 1822, immediately prior to intensive agricultural development, is recorded along section lines in General Land Office (GLO) survey data. Assessment of lateral migration of the bend more recently, under the condition of intensive agricultural development in the watershed, was conducted by analyzing change in the centerline position of the river channel between 1822 and 2022 using GLO data, georeferenced aerial imagery, and lidar-derived DEM data. Analysis of changes in river-channel centerline positions using historical data is a common method for determining movement of meander bends over timescales of several decades to centuries (Downward et al., 1994; Hughes et al., 2006; Kessler et al., 2013; Lea and Legleiter, 2016; Donovan et al., 2019).

3.1. Collection of floodplain cores

To estimate the long-term rate of lateral migration of the channel, the positions of scroll bars along the meander bend on the Sangamon River floodplain were first identified using a high-resolution (4 points or greater per square meter) lidar digital elevation model (DEM) obtained through the Illinois Height Modernization program (https://clearinghouse.isgs.illinois.edu/data/elevation/illinois-height-modernization-ilhmp). Six eight-meter cores with a diameter of 8 cm were extracted using a GeoProbe DT325 (Fig. 2) close to crests of scrolls bars along a transect extending 152 m from the inner bank of the river channel (Fig. 1). Collection of cores began in June 2021 and was completed in September 2021. The collected cores were sealed in plastic liners and stored under refrigeration at the Geological Samples Library of the Illinois State Geological Survey to prevent alteration of dateable carbonaceous material.

3.2. Core interpretation, facies identification, and particle-size analysis

The cores were examined for obvious changes in color; grain texture, sorting, structure, and rounding; degree or type of stratification; degree of oxidation; evidence of carbonate minerals (reactivity to acid); and presence of organic matter. The goal was to identify distinct sedimentary facies within the floodplain deposits as well as datable organic-matter samples like leaves, wood, and shells. Core characterizations supported interpretations of depositional environment and identification of facies thickness. Of particular interest in the present study is the distinction between overbank deposits produced by vertical accretion of fine sediment and lateral-accretion deposits produced by addition of sediment to the face of the point bar as the river migrates laterally. The



Fig. 2. Geoprobe coring at Allerton Park, September, 2021.

classic facies profile of a meandering-river floodplain consists of finegrained vertical-accretion deposits overlying coarse-grained lateral-accretion deposits (Rhoads, 2020). Identification of the depth at which the transition from lateral to vertical accretion occurs is important for defining sedimentological facies in which the age of deposits should decrease vertically (overbank deposits) versus those which age should decrease laterally (lateral-accretion deposits).

To aid in facies characterization, grain-size analysis was conducted on samples of material characterized as vertical-accretion and lateral-accretion deposits in cores 4A and 5B. Approximately 25 g of the fine-grained vertical-accretion deposits and 200 to 500 g of the sandy lateral-accretion deposits were collected. The fine-grained vertical-accretion deposits and lateral-accretion deposits that contained abundant (10 to 50 %) fines as determined from the USDA soil texture procedure (https://www.nrcs.usda.gov/sites/default/files/2022–11/texture-by-feel.pdf) were analyzed using laser diffraction. Samples were disaggregated and 5 g of the total sample material was then bleached and placed in hot water at 80 °C for 15 min to oxidize the organic matter. The samples were centrifuged for 10 mins at 2000 rpm to separate the

organic matter from the sediment. The processed samples were dried,

suspended in deionized water with dispersant, and shaken in a mini vortex mixer. The particle-size distribution of the suspended, dispersed sample was determined using a Malvern Mastersizer 3000 HydroEV. Samples that consisted almost entirely of sand and fine gravel were disaggregated using a mortar and pestle and the entire sample was sieved at one-half phi intervals over the range of 2 to 32 mm to determine different fractions of gravel. The pan fraction was then subsampled to obtain 100 to 150 g of material that was sieved at one-half phi intervals over the size range of 0.063 mm to 2.0 mm to determine different fractions of sand. Material remaining in the pan is the fraction of silt and clay.

3.3. Collection and radiocarbon dating of carbonaceous material

Samples of datable carbonaceous material, including leaves or wood (Cores 1B and 2A) and shells of the aquatic gastropod *Pleurocera acuta* (Cores 3A to 6A), were collected from the lateral-accretion deposits. Wood and leaf samples were $> 1~{\rm cm}^3$ in volume, and typically much larger than this minimum volume. All samples were well preserved; gastropod shells were intact and unbroken.

The samples were sent to the University of California, Irvine's Keck Carbon Cycle Accelerator Mass Spectrometer Laboratory for radiocarbon (14C) dating. Prior to combustion, wood and leaves were washed to remove sediment, followed by treatment with acid-base-acid (1 N HCl and 1 N NaOH, 75 $^{\circ}$ C). Shell samples were sonicated in water and then treated with dilute (10 %) HCl prior to hydrolysis with 85 % phosphoric acid to remove any adhering sediment or diagenetic carbonate coatings, such as dolomite or calcite. The carbon in the samples was converted to graphite by standard facility procedures and analyzed for radiocarbon abundance. Sample preparation backgrounds were subtracted, based on measurements of ¹⁴C-free wood (organics) and calcite (carbonates). All results have been corrected for isotopic fractionation according to the conventions of Stuiver and Polach (1977), with δ^{13} C values measured on prepared graphite using the AMS spectrometer. Radiocarbon contents were provided as Fraction Modern values, Δ^{14} C, and conventional radiocarbon age (Stuiver and Polach, 1977).

Past work has demonstrated that dating of gastropod shells can provide robust age control on terrestrial or fluvial deposits (Pigati et al., 2010; Rakovan et al., 2013). For freshwater aquatic shells, an age offset correction has been successfully applied to the raw ¹⁴C-content of shells to compensate for the reservoir age of carbonate in the river (Rech et al., 2023). The present study applied an age offset correction of 1490 yrs based on analyses of Sangamon River valley Pleurocera acuta shells obtained from the Illinois Natural History Survey archived collections. This correction is slightly higher than the 500-1000 year reservoir effect noted in southwestern Ohio for other species of freshwater mollusks (Rech et al., 2023). The six shells used for the correction were collected in 1912 in Champaign County, IL and in 1887 in McLean County, IL. No age offset correction was applied to the wood and leaves. To account for historical variations in atmospheric ¹⁴C levels, radiocarbon calibrations were performed using CALIB rev. 8 (Stuiver and Reimer, 1993; http ://calib.org/calib/ CALIB version 8.2html). The IntCal correction was used for Northern Hemisphere terrestrial samples.

3.4. Surveying of channel cross section and bed-material sampling and analysis

To compare the depth of lateral-accretion deposits in the floodplain to channel depth and to explore similarities and differences between channel sediments and floodplain sediments, a cross section of the river was surveyed at the study bend and samples of river-channel bed and bank materials were collected along this cross section. A rod-and-level survey was conducted to obtain the absolute elevations of both the banks and the channel bed. Sediment samples were collected from the upper 10–15 cm of the channel bed and banks. Bank samples, which contained abundant fines, were analyzed using laser diffraction

(Malvern Mastersizer 3000) to determine particle-size distributions, whereas bed material, which consisted mostly of sand and fine gravel, was sieved.

3.5. Historical analysis of channel change

Historical analysis of change in the centerline of study bend was based on three types of data: General Land Office Survey (GLO) records, aerial photography, and a high-resolution digital elevation model (DEM) derived from an airborne lidar survey. The GLO records include field notes of section-line surveys conducted as part of the Public Land Survey System. The study bend lies at the intersection of sections 20, 21, 28, and 29 in T18N R5E of the 3rd Principal Meridian. Field notes of surveys in 1822 of section lines that cross the Sangamon River are available through the National Archives Catalog, Record Group 49: Records of the Bureau of Land Management, within the series Field Notes for Public Land Survey Township Plats, Illinois: Volume 63–66. The field notes include distances from section-line endpoints to the banks of the Sangamon River as well as measurements of river width. The section-line distances plus one-half of the river width approximates the location of the channel centerline.

The earliest aerial image of the study bend is from July 1940 (USDA AM-5A-16). This unrectified image, downloaded from the Illinois State Geological Survey (ISGS) Geospatial Data Clearinghouse (https://clearinghouse.isgs.illinois.edu/), has a scale of about 1:20000 and was georeferenced using a 2021 orthoimage of Piatt County, IL. The orthoimage obtained as part of the United States Department of Agriculture's (USDA) National Agricultural Imagery Program (NAIP), was downloaded from the USDA Geospatial Data Gateway https://datagateway.nrcs.usda.gov/). It has a resolution of 60 cm. Geoferencing of the 1940 image was performed in in ArcPro 3.0 using 10 control points and a second-order polynomial transformation. Average root mean square error (RMSE) of the geoferencing was 1.75 m.

The lidar-derived DEM of Piatt County, which is based on airborne lidar scans flown in May and June 2022, was accessed through the ISGS Geospatial Data Clearinghouse. The positional accuracy of the lidar DEM is less than one meter. The aggregate nominal pulse density is 4 points or greater per square meter.

The channel centerline of the Sangamon River at the study bend was determined for the lidar DEM by digitizing as polylines the left and right boundaries of the hydro-flattened surface of the river and then applying the Collapse Dual Lines to Centerline tool in ArcPro 3.0. Lack of visibility of the channel banks or edge of water on the 1940 aerial image, which was obtained during leaf-on conditions, necessitated manual digitization of the river path. Only a narrow swath of the river surface about 6-12 m wide was visible on the 1940 imagery because of the dense forest canopy, and the centerline of this swath may not correspond with the true channel centerline. To assess potential error associated with leaf-on conditions, the channel centerline was digitized manually on the 2021 orthoimage, also obtained during leaf-on conditions, and this centerline was compared to the centerline generated for the 2022 lidar DEM. This analysis showed that error in centerline position related to canopy cover was as great as \pm 12 m. Differences in the positions of the centerlines were determined using the measurement tool in ArcPro 3.0 and these differences were divided by time to determine migration rates.

4. Results

4.1. Characteristics of floodplain deposits

All six cores have an upper layer consisting of very dark brown (Munsell 10YR 2/2 or 3/2), fine sediment dominated by silt and containing varying amounts of organic carbon (0.1–7 % by dry weight) (Fig. 3). This layer extends to a depth of about 1.0–1.3 m. Particle size analysis of the layer in core 5B shows that it consists mainly of silty clay loam and silt loam with clay content of 15–35 %, silt content of 60–70 %,



Fig. 3. Photograph of core 4A from the surface (upper right) to a depth of 3.35 m (lower left). Very dark brown, fine-grained overbank deposits in the upper 1.3 m (first two sections) overlie lateral-accretion deposits consisting of pale brown fine sand and dark brown loamy sand.

and sand content of < 5-15 % (Fig. 4). This upper layer is interpreted as overbank deposits that have accumulated on the floodplain surface mainly through vertical accretion (Figs. 4 and 5). Sediment below the upper layer transitions either into dark grayish brown to pale brown fine sand (> 95 % sand) (Fig. 3, Fig. 4, core 4A, 1.3-1.5m) or a dark brown loamy sand (\geq 80 % sand) (Fig. 4, core 5B, 1.2–1.5 m). Locally, interbedded layers of silt loam (25-30 % sand) are sometimes present (Fig. 4, core 5B, 1.8–2.1 m). This layer of sediment below the overbank deposits is interpreted as point-bar deposits that have accumulated through lateral accretion (Fig. 5). This interpretation is supported by analysis of the particle-size characteristics of river bed and bank material at the study bend. The inner bank of the meander bend generally consists of loam and sandy loam with clay content of 5-10 %, silt content of 20-55 %, and sand content of 45-80 % (Fig. 4), whereas bed material is composed primarily (>95 %) of sand and fine gravel (Fig. 4). The textural characteristics of the lateral-accretion deposits overall are quite similar to those of the bank and bed material of the modern river (Fig. 4), suggesting that these deposits indeed formed from accretion of bank and bed material onto the point bar of the meander bend as the channel shifted laterally across the floodplain.

4.2. Radiocarbon ages of leaves, wood, and shells in lateral-accretion deposits

A total of 14 datable samples consisting of shells, leaves and wood fragments were obtained from the lateral-accretion deposits (Table 1, Fig. 5). All shells are *Pluerocera acuta* (Fig. 6). Dates of organic materials range from 100 yrs BP (before 1950) for a wood fragment in core 2A to 4120 years BP for a shell in core 3A. Distances of the cores from the inner bank of the river range from 13 m at core 1B to 152 m at core 6A (Table 1; Fig. 5). When plotted by age versus distance, the age of the samples generally increases with distance, except for samples 3A-1 and 3A-2, which have large ages relative to their distance from the inner bank (Fig. 7a). These two samples have dates considerably older than dates of samples at about the same elevation in adjacent cores and of an underlying sample from the same core (Fig. 5). They appear to be outliers that represent old shells deposited within much younger material. If these ages are omitted, regression analysis of age versus distance from the inner bank yields an average rate of lateral movement of the bend of 0.052 m/yr (R² = 0.86) (Fig. 7a). Rates corresponding to 95 % confidence intervals of this analysis are 0.045 m/yr and 0.089 m/yr. The age of sample 6A-2 (3820 yrs BP) can be considered a possible outlier because shells above and below this sample have much younger ages (> 1600 yrs). If sample 6A-2 is excluded from the regression analysis, the average rate of migration increases slightly to 0.064 m/yr with confidence intervals of 0.044 m/yr and 0.087 m/yr (Fig. 7B).

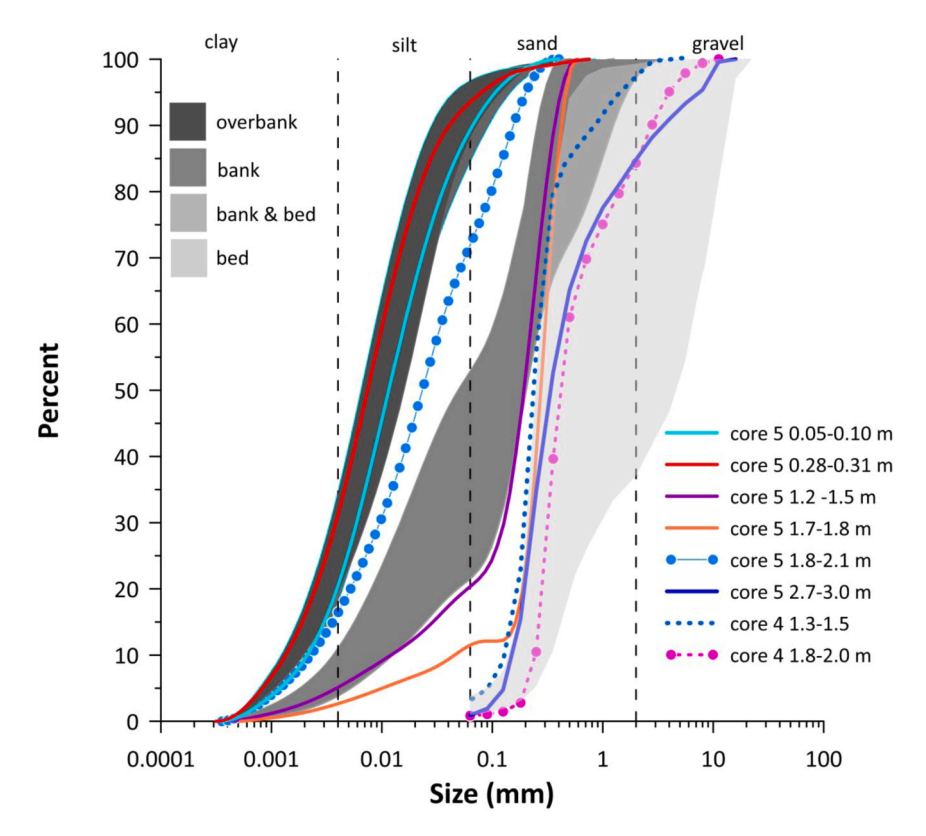


Fig. 4. Particle size domains of overbank, riverbank and riverbed (overlap), and riverbed sediments in the Sangamon River channel and floodplain at the study bend. Cumulative distribution curves are shown for samples from cores 4A and 5B. Dotted lines indicate sediment samples that include shells with radiocarbon dates.

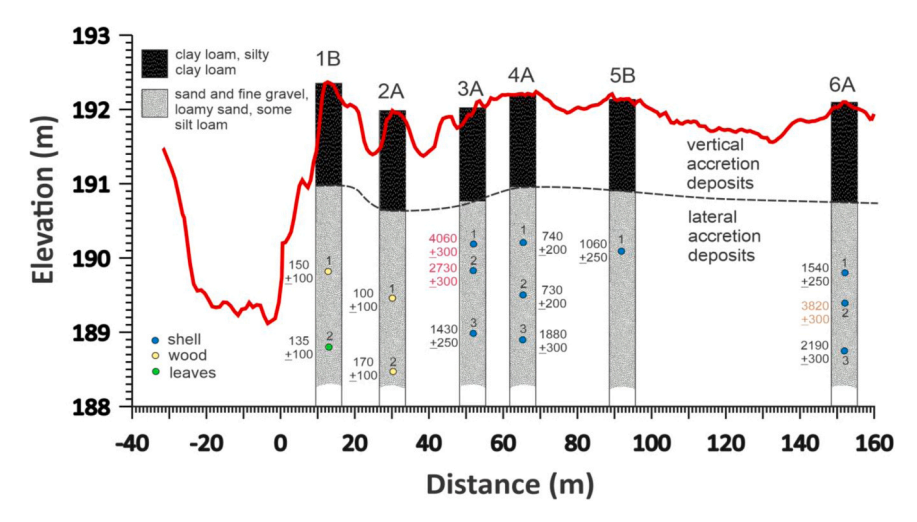


Fig. 5. Transect across study bend from inner channel bank (0 m) to outer channel bank (negative distances) and to locations of cores on the floodplain within the bend (positive distances). Interpretated vertical-accretion (overbank) deposits and lateral-accretion deposits are indicated for each core. Also shown are the positions, types, and dates of samples used to determine lateral migration rates.

The process of lateral accretion should produce deposits that are time-transgressive at approximately the same elevation across the floodplain, assuming that the river is neither incising or aggrading substantially over the timescale under consideration. Further exploration of possible migration rates using the sample dates is conducted on the basis of this assumption. Including only the dates of samples between elevations of 189.5 m and 192.2 m in the regression analysis, except for the two outliers in core 3A, results in an average migration rate of 0.095 m/yr with confidence intervals of 0.087 m/yr and 0.108 m/yr (Fig. 7C). Considering the dates of samples in the lateral-accretion

deposits below an elevation of 189.5 m, produces an average migration rate of 0.045 m/yr with confidence intervals of 0.035 m/yr and 0.070 m/yr (Fig. 7D). Excluding the date for sample 6A-2, a possible outlier, changes the average migration rate to 0.051 m/yr with confidence intervals of 0.035 and 0.118 m/yr (Fig. 7E).

Collectively, these different analyses of the core-sample dates suggest that the migration rate of the bend has been between 0.035 and 0.12 m/yr with the average rate most likely around 5 to 9 cm/yr. Given that the bankfull width of the river at the study bend is about 30 m, the average rate of lateral migration over the timescale of bend migration

Table 1 Characteristics of dated samples in cores 1–6.

Core- Sample	Material	Depth (m)	Depositional Material	Distance from Inner Bank (m)	Calibrated Age \pm 2 σ (Years Before 1950)
1B-1	Wood	2.68	Very fine to fine sand, horizontal bedding	13	150 ± 100
1B-2	Leaves	3.57	Fine sand with interbedded silt, horizontal bedding	13	135 ± 100
2A-1	Wood	2.65	Silt loam with fine sand	30	100 ± 100
2A-2	Wood	3.57	Laminated silt	30	170 ± 100
3A-1	Shell Pleurocera acuta	1.83	Sand with some fine gravel and silt	52	4060 ± 300
3A-2	Shell Pleurocera acuta	2.13	Fine to coarse sand with some silt	52	2730 ± 300
3A-3	Shell Pleurocera acuta	3.05	Fine to coarse sand, some fine gravel	52	1430 ± 250
4A-1	Shell Pleurocera acuta	1.98	Fine to coarse sand with some fine gravel	65	740 ± 200
4A-2	Shell Pleurocera acuta	2.74	Fine to coarse sand with some fine gravel	65	730 ± 200
4A-3	Shell Pleurocera acuta	3.35	Sand and gravel with some silt	65	1880 ± 300
5B-1	Shell Pleurocera acuta	1.98	Silt loam with fine sand	92	1060 ± 250
6A-1	Shell Pleurocera acuta	2.29	Sand with some silt	152	1540 ± 250
6A-2	Shell Pleurocera acuta	2.74	Sand and fine gravel	152	3820 ± 300
6A-3	Shell Pleurocera acuta	3.35	Sand and fine gravel	152	2190 ± 300



Fig. 6. Pleurocera acuta gastropod shell from Core 5B. Scale in centimeters.

has been about 0.2 % to 0.3 % of the channel width per year. The timescale of migration recorded in the scoll bars is somewhat uncertain. The dates of material in core 6A range from 1540 \pm 250 yrs to 3820 \pm 300 yrs. Similarly, the best-fit lines of the regression analyses yield dates at 152 m (distance to core 6A) ranging from 1600 yrs to 3400 yrs. The relative consistency of two dates in core 6A (6A-1 and 6A-3, Fig. 4) and regression analyses that exclude samples 3A-1, 3A-2, and

6A-2 provide support for a timescale between 1580 and 2190 yrs.

4.3. Historical channel change

Comparison of channel centerline positions of the study bend for the GLO records, 1940 georeferenced image and the 2022 lidar DEM reveals that the centerline appears to have shifted slightly over the 200-year period of analysis (1822–2022) (Fig. 8). The four locations of the channel centerlines as determined from the 1822 GLO surveys are within 10 m or less of the 1940 and 2022 centerlines near the bend entrance and exit (Table 2). Near the bend apex, the 1822 centerline locations (SL2 and SL3) deviate from the positions of the other two centerlines by 11 to 27.5 m (Table 2). Assuming the position of the 1940 centerline is accurate, rates of migration of the river between 1822 and 1940 at the four section-line crossings range from 0.233 m/yr for SL3 to 0.076 m/yr for SL4 (Table 2).

Differences between the 1940 and 2022 centerlines within the study bend vary from 0 m (overlap) to about 10 m based on perpendicular lines of displacement between the centerlines. Immediately upstream of the apex of the bend, the 2022 centerline locally lies between one and ten meters farther toward the inner bank of the bend (i.e. to the west) compared to the 1940 centerline (Fig. 8). At the apex, where the channel curves most sharply, the two centerlines coincide closely with one another. In the downstream limb, the 2022 centerline is positioned between one and nine meters to the southwest compared to the 1940 centerline. The outward (southwestward) shift of the centerline in the downstream limb of the bend, the lack of change in centerline near the bend apex, and the inward (westward) shift of the centerline upstream of the apex are suggestive of a possible rotational pattern of bend evolution (Fig. 8).

Maximum displacement of $10\,\mathrm{m}$ over the 82-year period (1940–2022) equates to a maximum migration rate of $0.12\,\mathrm{m/yr}$. The average migration rate, obtained by dividing areas of change between the two centerlines (2400 m²) by the distance along the centerline through the bend (480 m) is $0.05\,\mathrm{m/yr}$. Locally, migration rates vary from a minimum of zero (no change) to the maximum rate of $0.12\,\mathrm{m/yr}$.

Including displacement between the 1940 and 2022 centerlines in estimation of migration rates between 1822 and 2022 at the four section-line crossings results in rates ranging from 0.165 to 0.070 m/yr (Table 2). These rates, along with the estimated migration rates from 1822 to 1940, are uncertain. The maximum difference between the 1940 and 2022 centerlines (12 m) equals or slightly exceeds the maximum difference between the 2021 and 2022 centerlines (Fig. 8), which was used to estimate centerline uncertainty for the 1940 centerline. The centerline for 2022 lies entirely within this band of uncertainty around the 1940 centerline (Fig. 8), indicating that when considering possible error, the two centerlines cannot be definitively distinguished from one another. Thus, while differences between the centerlines can be measured and converted to migration rates, estimates of migration rates for 1822-1940 and 1940-2022 may contain substantial error. Comparing channel centerline positions at the four section-line crossings for 1822 and 2022 only, i.e. not including information for the 1940 centerline, results in migration rates ranging from 0.125 m/yr to 0.018 m/yr (Table 2).

5. Discussion

The analysis of radiocarbon-dated samples indicates that over a period of a few thousand years, the study bend along the Upper Sangamon River has migrated on average about 0.05 to 0.10 m/yr, or 0.2 to 0.3 % of its contemporary width. This rate is low for an alluvial river. When plotted on a cumulative frequency curve of lateral migration rate per unit width based on 937 measurements of bank erosion and channel migration for 336 rivers and streams throughout the world (Rowland and Schwenk, 2019), the migration rate for the Sangamon River is equaled or exceeded by 92–94 % of the data (Fig. 9). This relatively low

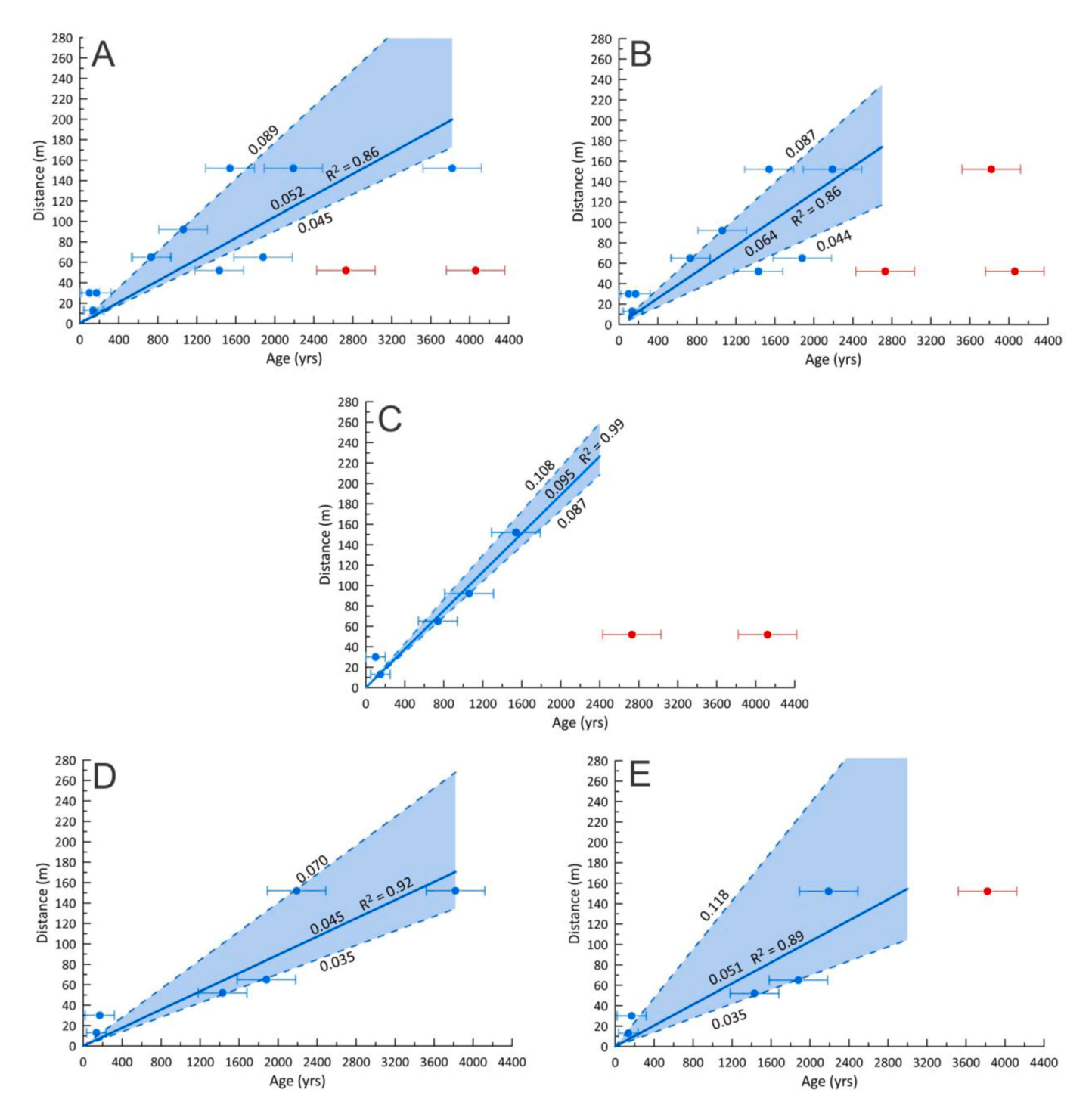


Fig. 7. Regression analyses of age versus distance. A. All ages except for two outliers in Core 3A (3A-1 and 3A-2). B. All ages except for two outliers in Core 3A (3A-1 and 3A-2) and a possible outlier in Core 6A (6A-2). C. Ages between 189.5 and 196.2 m, excluding the two outliers in Core 3A. D. All ages for elevations below 189.5 m. E. All ages below 189.5 m, excluding possible outlier in Core 6A. Uncertainties associated with individual radiocarbon dates shown as error bars. Red symbols denote outliers excluded from regression analyses. Confidence intervals (± 95 %) of regression analyses shown by blue shading.

rate of lateral migration occurred well prior to European settlement of the watershed upstream of the study bend in the 1800s and the wide-spread implementation of tile drainage and surface drainage ditches in the late 1800s to early 1900s (Rhoads et al., 2016).

Historical rates of lateral migration since 1822 exhibit variability in conjunction with treatment of uncertainty for the 1940 centerline. Change in the centerline between 1822 and 1940 yields migration rates of 0.186 m/yr (SL2) and 0.233 m/yr (SL3) (Table 2) for the part of the bend near the apex – values that locally are higher than the range of

0.035 to 0.11 m/yr for the long-term migration rate derived from the radiocarbon analysis. Thus, rates of migration of part of the study bend may have been higher than long-term average rates during agricultural development of the Sangamon River watershed. The average rate of migration between 1940 and 2022 (0.05 m/yr) – a period marked by widespread implementation of soil-conservation practices – is similar to the average long-term rate ($\approx\!0.06$ m/yr), suggesting that migration has slowed somewhat relative to 1822–1940 . Including the 1940 centerline in estimates of migration over the past 200 years yields values near the

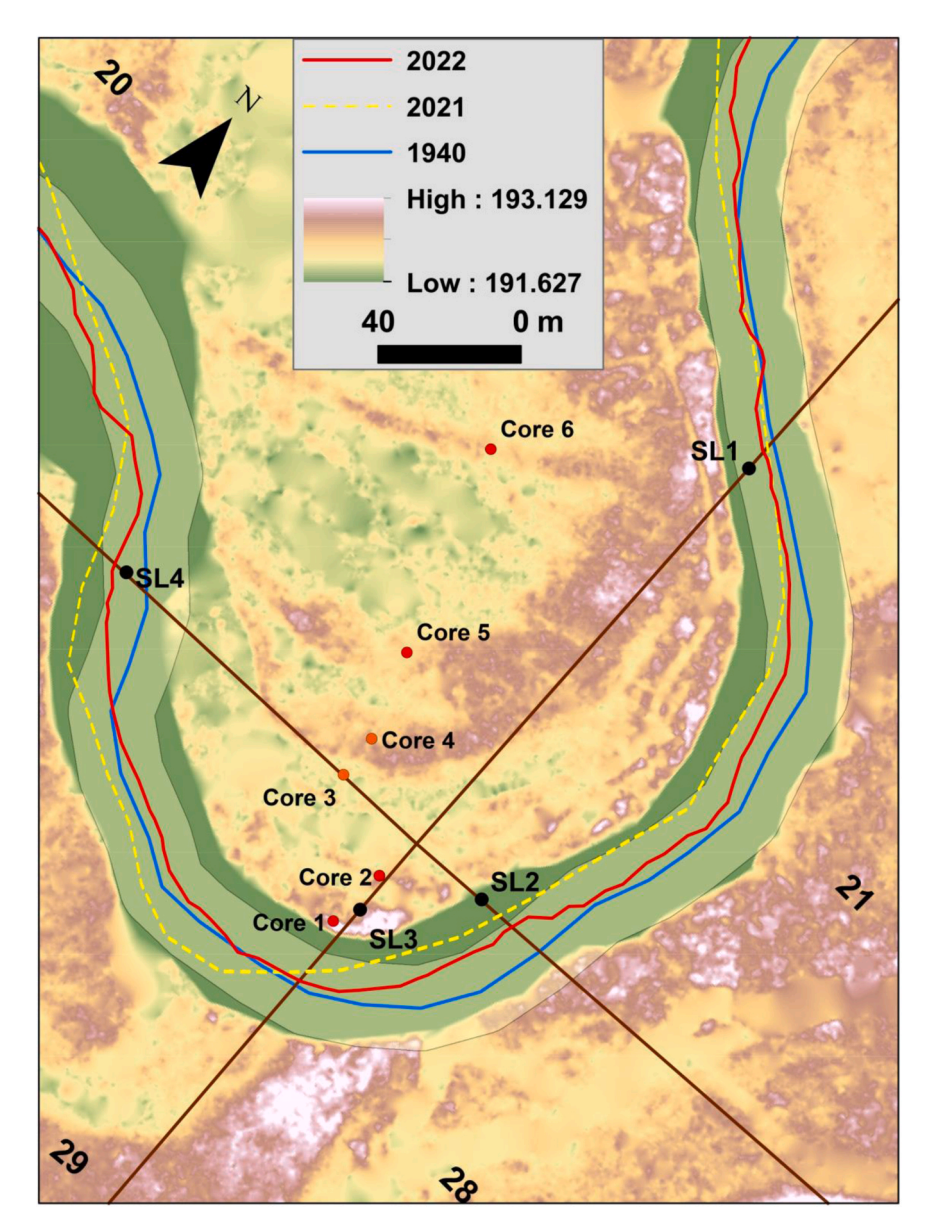


Fig. 8. Channel centerline positions of 1822 and 2022 for the study bend (superimposed on 2022 lidar DEM). 1822 positions (SL1, SL2, SL3, SL4) are shown as discrete locations along section lines corresponding to the GLO survey notes. 2021 leaf-on orthoimage centerline is included for comparison with lidar DEM 2022 centerline. Section lines are shown in brown and section numbers in bold black. Light green shading is \pm 12 m error band around the 1940 centerline.

Table 2GLO data from 1822 for section lines crossing the study bend on the Sangamon River.

				0	,	0				
Location	Distance to Riverbank from Intersection of Secs. 20, 21, 28, 29		Chann Width		Distance to River Centerline (CL)	1822-1940 CL Diff.	1822-2022 CL Diff.	Est. Mig. Rate 1822-1940	Est. Mig. Rate 1822-2022 [#]	Est. Mig. Rate 1822-2022*
	chains	m	links	m	m	m	m	m/yr	m/yr	m/yr
SL1 (sects. 20 & 21)	6.27 (E bank)	126	150	30	141	10	6	0.085	0.070	0.030
SL2 (secs. 21 & 28)	0.5 (N bank)	10	150	30	25	22	11	0.186	0.165	0.055
SL3 (secs. 28 & 29)	1.8 (S bank)	36	150	30	21	27.5	25	0.233	0.148	0.125
SL4 (secs. 20 & 29)	4.74 (E bank)	95	170	34	112	9	3.5	0.076	0.108	0.018

[#] estimated from sum of differences in positions of centerlines 1822-1940 and 1940-2022

^{*}estimated from differences in positions of centerlines 1822-2022 (excluding 1940).

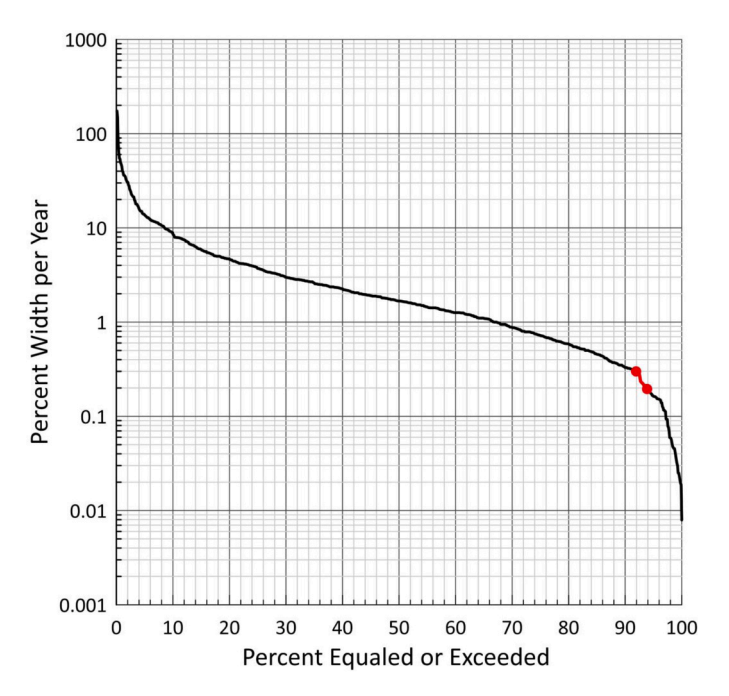


Fig. 9. Cumulative frequency curve of the rate of bank erosion per year expressed as the percent of channel width based on 937 measurements for 336 rivers around the world (Rowland and Schwenk, 2019). Red dots and line show estimated range of average migration rates of the study bend along the Sangamon River in Allerton Park.

apex (SL2 and SL3) that locally exceed maximum rates from the radiocarbon analysis by about 30 to 40 % (Table 2).

Because the error band of the 1940 centerline encompasses the 2022 centerline (Fig. 8), the 1940 centerline may not actually differ from the 2022 centerline. The outward shift of the 1940 centerline relative to the 1822 and 2022 centerline positions near the bend apex corresponds to a possible reversal of the direction of bend migration from toward the outer bank (1822-1940) to toward the inner bank (1940 to 2022) (Fig. 8). Such a shift in migration should produce a low depositional bench, known as a concave-bank bench, along the outer bank with a maximum elevation below the height of the floodplain next to the outer bank (Page and Nanson, 1982; Hooke and Yorke, 2011; Sylvester et al., 2021). Field observations at low flow and the lidar DEM, which is based on elevation data obtained at low flow, confirm that a depositional bench does not exist along the outer bank. Instead, the elevation of the floodplain along the outer bank is generally greater than the elevation of the floodplain along the inner bank - a configuration consistent with progressive migration of the river toward the outer bank (Lauer and Parker, 2008). These considerations support the inference that the difference between the 1940 and 2022 centerlines may largely reflect error related to leaf-on obscuration of the 1940 river channel. Ignoring the 1940 centerline yields estimates of lateral migration (0.018 -0.125 m/yr) between 1822 and 2022 that conform closely to the range of long-term migration rates determined from the dating of wood, leaves, and shells in lateral-accretion deposits (0.035 m/yr to 0.118 m/yr) (Table 2). The findings from this analysis imply that changes in watershed hydrology and sediment dynamics related to agricultural development have not substantially altered average rates of lateral migration of the study bend.

Radiocarbon ages of samples in cores 1B and 2A fall within the range of $100-170~\rm yrs$ before $1950~\rm (\pm 100~\rm yrs)$, suggesting that lateral-accretion deposits at the locations of these cores may be historical. This inference is consistent with the location of the channel centerline at SL2 and SL3 determined from the 1822 GLO records. The scroll bar corresponding to core 2A lies about $10-12~\rm m$ inward along the section lines that extend through SL2 and SL3 (Fig. 8). Given that the river width

in 1822 was reported as 30 m, this range of distances is remarkably close to a channel half-width of 15 m. Thus, the scroll bar corresponding to Core 2A likely represents the inner bank of the river in 1822. The scroll bar corresponding to Core 1B occurs at the top of the modern riverbank and would have developed or begun to develop when the river moved to its current position.

The similar dates of samples in cores 1B and 2A, the change in position of the river centerline between 1822 and 1940, and similarity in positions of the 1940 and 2022 centerlines indicate that the study bend shifted to its current position sometime between 1822 and 1940 at an accelerated rate. This argument is valid even if the 1940 centerline is considered identical to the 2022 centerline. Whether or not accelerated movement of the bend between 1822 and 1940 is the result of postsettlement changes in watershed conditions remains unclear. Rates of migration of meandering rivers typically exhibit high spatial and temporal variability even when environmental conditions are not dramatically affected by anthropogenic change (Hooke, 2022, 2023; Moody, 2022). Also, inner-bank deposition leading to the formation of scroll bars is an episodic process that depends on discharge and interaction of inner-bank deposition with outer-bank erosion (Kasvi et al., 2013; Ghinassi et al., 2019). Despite low average rates of migration of the bend derived from the radiocarbon analysis, movement of the river over the timescale of this analysis could have occurred in a highly episodic manner. Average rates do not provide information on the timescale over which shifts in position of the river truly occurred.

The change in river centerline from 1940 to 2022 either is small (assuming 1940 is accurate) or nearly zero (assuming the two centerlines are nearly equivalent). Average rates of migration over the past 200 years estimated by omitting the uncertain 1940 centerline (Table 2) are similar to the low long-term average rates derived from the radiocarbon analysis. These estimated rates over 200 years include change in centerline position that presumably occurred sometime between 1822 and 1940. Thus, the most reliable data in the historical analysis support the inference that low average rates of migration have persisted throughout the historical period, despite transformation of more than 80 % of the land in the watershed to agriculture. This transformation has increased drainage density three-fold through the addition and extension of channels in headwater portions of the watershed (Rhoads et al., 2016). The increase in drainage density, along with widespread removal of native prairie and implementation of tile drainage, has undoubtedly increased amounts and rates of runoff, but the magnitudes of these changes are difficult to quantify without information on pre-settlement hydrology. Historical information from the late 19th/early 20th century to the present shows that while mean annual precipitation has gradually increased, this increase is not reflected in the patterns of mean annual discharge or peak discharge over this period (Fig. 10). Available evidence does suggest that human-induced transformation Sangamon-River watershed has dramatically increased sediment fluxes. Evaluation of fly-ash content of overbank deposits on the floodplain at Allerton Park shows that vertical accretion rates have increased an order of magnitude since European settlement (Grimley et al., 2017). This large increase in vertical accretion signals a major change in the fine sediment load of the river system, presumably related to high rates of agricultural soil erosion since the mid-1800s. Such a finding is consistent with modeling results that predict eleven-fold greater rates of soil erosion and eight-fold greater river sediment loads today than in the early 1800s for identical runoff-producing precipitation events (Yu, 2018).

The lack of verifiable lateral migration of the study bend since 1940 is consistent with previous network-scale analysis of lateral migration of streams throughout the upper Sangamon River basin between 1940–41 and 2012 (Rhoads et al., 2016). This previous analysis did not quantify lateral erosion rates, but it did determine that the Sangamon River downstream of Monticello, IL, including the portion of the river in Allerton Park, exhibited no detectable change at a resolution of one-channel width of displacement. Meander migration equal to 3 to 4

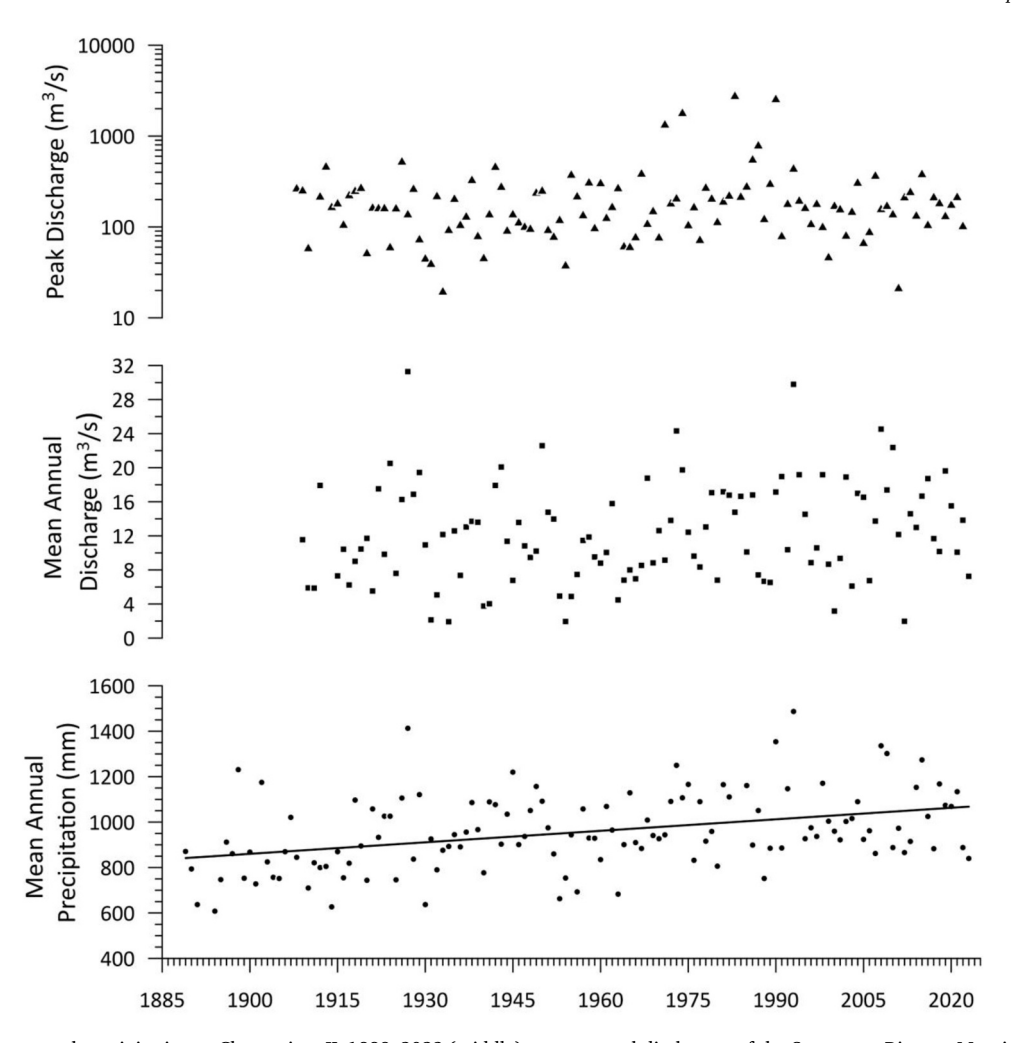


Fig. 10. (bottom) mean annual precipitation at Champaign, IL 1889–2023 (middle) mean annual discharges of the Sangamon River at Monticello 1909–2023 (top) peak discharges of the Sangamon River at Monticello 1909–2023.

times the channel width was documented in headwater portions of the Sangamon River and in its tributaries, particularly in areas of floodplain grazing (Rhoads, 2016). In these portions of the watershed, eroded bank material is a major source of suspended sediment (Neal and Anders, 2015; Yu and Rhoads, 2018).

Factors that impede high average rates of lateral migration of the upper Sangamon River include cohesive riverbanks, root reinforcement of these riverbanks by trees, abundant large wood in the river channel



Fig. 11. Aerial image of the Sangamon River near the apex of the study bend showing abundant woody debris in the river channel and tree-lined banks. Looking downstream – inner bank to the right and outer bank to the left.

that increases flow resistance (Fig. 11), and low bankfull stream power per unit area of the river. Together, resistant banks and low fluvial energy constrain erosion of outer banks and the corresponding deposition of sediment on point bars along inner banks that drives lateral migration (Candel et al., 2020). High cohesion increases bank strength and resistance to erosion as does root reinforcement of channel banks by riparian vegetation (Polvi et al., 2014; Konsoer et al., 2016; Yu et al., 2020; Dawson and Lewin, 2023). Resistance to erosion can be increased by an order of magnitude by these combined effects. The magnitude of increase in river discharges caused by agricultural development in the Sangamon Basin is unknown, but likely was substantial compared to presettlement conditions when runoff was inhibited by prairie grass and movement of water into the river system was not enhanced by tile drains and drainage ditches (White et al., 2003; Kelly et al., 2017). Although discharge, or its surrogate, drainage area, has been viewed as an important factor influencing rates of meander migration (Hooke, 1980, 1987) and changes in discharge have been associated with changes in meander migration rates (Schook et al., 2017; Candel et al., 2018; Moody, 2022), not all meandering rivers are sensitive to changes in discharge (Donovan and Belmont, 2019). Although enhanced post-agricultural overbank deposition has possibly increased channel depth by about 25 % (0.8 m), this change in channel form is unlikely to affect rates of lateral migration because bank erosion in this river system is caused mainly by mobilization of noncohesive sand and gravel deposits at the base of the banks.

Because stream power depends on discharge, increases in discharge caused by agricultural development will also increase stream power.

Bankfull stream power per unit area (ω_h) (W/m^2) is:

$$\omega_b = \gamma Q_b S / W \tag{1}$$

where γ is the specific weight of water (assumed to be 9810 N/m³) Q_h is the bankfull discharge (m^3/s) , S is channel slope (m/m), and W is channel width (m). Previous hydraulic analysis of the Sangamon River at Allerton Park has shown that the bankfull discharge is about 45 m³/s (Lindroth et al., 2020). This value, along with a channel slope of 0.00026 and bankfull width of 30 m, yields $\omega_b = 4 \text{ W/m}^2$. The low contemporary bankfull stream power per unit area of the Sangamon River implies that any increases in discharge associated with agricultural development have not greatly elevated the magnitude of ω_b . Meandering streams in portions of Illinois and Indiana that were glaciated during the Wisconsin Episode exhibit negligible lateral migration and can require a century or more to recovery their sinuosity if artificially straightened when bankfull stream power per unit area is less than 25 W/m² (Urban and Rhoads, 2003; Güneralp and Rhoads, 2009; Salas and Rhoads, 2022). Similarly, channelized rivers in lowland glaciated environments of Europe typically respond minimally to channelization when $\omega_b < 35 \text{ W/m}^2$ (Brookes, 1987a; b). The value of ω_b for the Sangamon River is an order of magnitude less than this threshold so a slow rate of lateral migration is to be expected.

Tthe Sangamon River, a low-gradient meandering river situated in a landscape glaciated as recently as 22,000 years ago, appears to have responded to watershed-scale agricultural impacts similarly to lowgradient rivers in unglaciated portions of the Midwest. The low rate of meander migration of the Sangamon River at Allerton Park is consistent with previous work on meandering rivers in the Driftless Area that has indicated power per unit area must exceed 30 W/m² for incised streams to exhibit substantial lateral migration over the time span between the middle of the 20th century and the end of the 20th century (Lecce, 1997). Influxes of sediment to downstream portions of the Sangamon River system from soil erosion have led to vertical accretion of floodplains but have not strongly influenced river lateral migration rates, as has been the case in the Driftless Area (Knox, 1987; Lecce, 1997). Although increases in suspended sediment flux have been associated with increased rates of lateral migration in meandering rivers (Constantine et al., 2014; Ahmed et al., 2019; Donovan et al., 2021), it seems likely that this relationship reflects an increase in suspended bed-material load (sand), rather than wash load (silt and clay). The transport of wash load is essentially independent of hydraulic conditions in river and should not have a major influence on erosion and deposition of alluvial channel boundaries (Rhoads, 2020). The fine-grained nature of overbank deposits indicates that most suspended material in the Sangamon River is silt or clay, which constitutes wash load. Moreover, the relationship between suspended sediment flux and bank erosion has recently been called into question by a global analysis of riverbank erosion, which failed to find strong relationships between these two variables for most major rivers systems of the world (Langhorst and Pavelsky, 2023).

Sources of uncertainty in the study include possible inaccuracy of leaf, wood, and shell dates and error in GIS-based analysis of channel change. Every effort has been made to conform to accepted standards for radiocarbon dating of samples and in consideration of age adjustments. Although gastropod dates were adjusted to accommodate reservoir effects, at least two shells have dates that deviate substantially from those for other samples. Possible reworking of older shells is difficult to verify, but relations among the ages of samples can provide a reasonable basis for identifying outliers likely related to reworking. The analysis has considered different types of age-distance relations to explore variability in estimates of rates of lateral migration and in the timescale of migration. Additional dating of sands in the lateral-accretion deposits using OSL methods may help to clarify the migration chronology of the bend.

Another source of uncertainty is whether migration occurred consistently in the same direction over the timescale of analysis or

whether reversals in migration direction might have happened (Donovan and Belmont, 2016). Reversals within an interval of channel-change analysis, i.e. between successive aerial images/lidar scans or between episodes of deposition that produce dated lateral-accretion deposits, will lead to underprediction of actual migration rates. Accurate detection of reversals between 1822 and 2022 is complicated by uncertainty in the 1940 centerline. The position of the 1940 centerline relative to the 1822 and 2022 centerlines indicates that the pattern of migration may have reversed at some positions around the bend in or prior to 1940 (Fig. 8); however, this apparent reversal may simply reflect error in the 1940 centerline. Possible reversals are accounted for in the historical analysis of planform change by assuming the 1940 centerline is accurate (Table 2).

6. Conclusion

Dating of organic material in lateral-accretion deposits as well as analysis of channel change over a 200-year period for a meander bend along the Sangamon River, a lowland meandering river in the midwestern United States, show that average rates of lateral migration determined from the most reliable available data are similar before and after agricultural development at the watershed scale. This similarity suggests that agricultural development has not substantially changed the migration dynamics of this meandering river. Average rates of migration are low (0.02 to 0.03 % of channel width) both before and after the implementation of agriculture. Although agriculture has increased runoff and sediment delivery to the river, average rates of lateral migration have not changed because other factors, including treelined riverbanks consisting of fine-grained cohesive sediment, abundant large wood in the river channel, and low bankfull stream power per unit area ($< 5 \text{ W/m}^2$), limit the capacity of the river to erode its banks. The low stream power of this river in part reflects the low relief of the watershed in which it is situated, the topography of which has been strongly influenced by glacial deposition during the late Wisconsin Episode. Nevertheless, the lack of increase in lateral migration of this river is broadly consistent with other studies in the agricultural Midwest, including work in the Driftless Area showing that lateral migration of meandering rivers is limited when bankfull stream power is less than 30 W/m². The constrained lateral migration of this river also conforms to findings that channel adjustment to artificial straightening in parts of the Midwest glaciated during the Wisconsin Episode occurs over timescales of decades to centuries when bankfull stream power per unit area is less than 25 W/m². Parts of the bend may have migrated at accelerated rates relative to the long-term average rate during the period that included clearing of native prairie for agricultural development (1822–1940), but this local movement of the bend cannot be definitively related to change in watershed land cover; it may simply reflect inherent variability in the process of meander migration.

From a management perspective, the results demonstrate the importance of riparian vegetation in maintaining the lateral stability of lowland meandering rivers. Maintenance of riparian forest along midwestern rivers limits lateral migration because the roots of large trees are highly effective in constraining bank erosion (Rood et al., 2015; Konsoer et al., 2016). Riparian forests also introduce large wood into rivers, which can mitigate bank erosion by increasing flow resistance (Dudley et al., 1998) and modifying patterns of flow through channel bends (Daniels and Rhoads, 2003, 2004), thereby increasing lateral stability (Brooks and Brierley, 2002). Thus, meandering rivers in forested areas have been shown to have lower rates of lateral migration than those that flow through cropland (Micheli et al., 2004; Zhu et al., 2022). In the Sangamon River basin, meander migration rates tend to be highest where forest vegetation has been disturbed or removed, such as in areas of grazing (Rhoads et al., 2016; Yu and Rhoads, 2018). The existence of a nearly continuous riparian corridor along the lower part of the upper Sangamon River, combined with its low stream power and fine-grained sediment load, probably accounts in large part for its low rates of lateral

migration.

CRediT authorship contribution statement

Dr. Neal Blair: Writing – review & editing, Validation, Investigation, Formal analysis, Data curation. Dr. Andrew Stumpf: Writing – review & editing, Methodology, Investigation, Formal analysis, Data curation. Dr. David Grimley: Writing – review & editing, Validation, Methodology, Formal analysis. Poushalee Banerjee: Writing – review & editing, Visualization, Validation, Methodology, Investigation, Formal analysis. Dr. Alison Anders: Writing – review & editing, Supervision, Methodology, Investigation, Funding acquisition, Formal analysis, Data curation, Conceptualization. Dr. Bruce Rhoads: Writing – review & editing, Writing – original draft, Visualization, Validation, Supervision, Resources, Project administration, Methodology, Investigation, Funding acquisition, Formal analysis, Data curation, Conceptualization.

Declaration of Competing Interest

The authors declare that they have no known competing financial interests or personal relationships that could have appeared to influence the work reported in this paper.

Data availability

Data will be made available on request.

Acknowledgements

Financial support was provided by the U.S. National Science Foundation (NSF) Grant # EAR-2012850 for the project Network Cluster CINET: Critical Interface Network in Intensively Managed Landscapes.

References

- Ahmed, J., Constantine, J.A., Dunne, T., 2019. The role of sediment supply in the adjustment of channel sinuosity across the Amazon Basin. Geology 47 (9), 807–810. https://doi.org/10.1130/g46319.1
- Anders, A.M., Bettis, E.A., Grimley, D.A., Stumpf, A.J., Kumar, P., 2018. Impacts of quaternary history on critical zone structure and processes: examples and a conceptual model from the intensively managed landscapes critical zone observatory. Front. Earth Sci. 6 https://doi.org/10.3389/feart.2018.00024.
- Baker, R.G., Bettis, E.A., Horton, D.G., 1993a. Late Wisconsinan-early Holocene riparian paleoenvironment in southeastern Iowa. Geol. Soc. Am. Bull. 105 (2), 206–212. https://doi.org/10.1130/0016-7606(1993)105<0206:lwehrp>2.3.co;2.
- Baker, R.G., Schwert, D.A., Bettis III, E.A., Chumbley, C.A., 1993b. Impact of Euro-American settlement on a riparian landscape in northeast Iowa, midwesten USA: an integrated approach based on historical evidence, floodplain sediments, fossil pollen, plant macrofossils and insects. Holocene 314–323.
- Beach, T., 1994. The fate of eroded soil sediment sink and sediment budgets of agrarian landscapes in southern Minnesota, 1851-1988. Ann. Assoc. Am. Geogr. 84 (1), 5–28. https://doi.org/10.1111/j.1467-8306.1994.tb01726.x.
- Belby, C., Spigel, L.J., Fitzpatrick, F.A., 2019. Historic changes to floodplain systems in the Driftless Area. In: Carson, E.C., Rawling, J.E., Daniels III, J.M., Attig, J.W. (Eds.), The Physical Geography and Geology of the Driftless Area: The Career and Contributions of James C. Knox. Geological Society of America Special Paper 543, Boulder, Co, pp. 119–145.
- Bigelow, D.P., Borchers, A., 2017. Major Uses of Land in the United States, 2012. U.S. Department of Agriculture, Economic Research Service.
- Blair, N.E., Hayes, J.M., Grimley, D., Anders, A., 2022. Eroded critical zone carbon and where to find it: examples from the IML-CZO. In: Wymore, A.S., Yang, W.H., Silver, W.L., McDowell, W.H., Chorover, J. (Eds.), Biogeochemistry of the Critical Zone. Springer, pp. 121–139.
- Brookes, A., 1987a. River channel adjustments downstream from channelization works in England and Wales. Earth Surf. Process. Landf. 12 (4), 337–351. https://doi.org/ 10.1002/esp.3290120402.
- Brookes, A., 1987b. The distribution and management of channelized streams in Denmark. Regul. Rivers 1, 3–16.
- Brooks, A.P., Brierley, G.J., 2002. Mediated equilibrium: The influence of riparian vegetation and wood on the long-term evolution and behaviour of a near-pristine river. Earth Surf. Process. Landf. 27 (4), 343–367. https://doi.org/10.1002/esp.332.
- Candel, J.H.J., Kleinhans, M.G., Makaske, B., Hoek, W.Z., Quik, C., Wallinga, J., 2018. Late Holocene channel pattern change from laterally stable to meandering - a palaeohydrological reconstruction. Earth Surf. Dyn. 6 (3), 723–741. https://doi.org/ 10.5194/esurf-6-723-2018.

- Candel, J.H.J., Makaske, B., Kijm, N., Kleinhans, M.G., Storms, J.E.A., Wallinga, J., 2020. Self-constraining of low-energy rivers explains low channel mobility and tortuous planforms. Depos. Rec. 6 (3), 648–669. https://doi.org/10.1002/dep2.112.
- Carson, E.C., Rawling III, J.E., Daniels, J.M., Attig, J.W., 2019. The Physical Geography and Geology of the Driftless Area: The Career Contributions of James C. Knox. GSA Special Paper 543. Geological Society of America, Boulder, CO.
- Clavijo-Rivera, A., Sanclemente, E., Altamirano-Moran, D., Munoz-Ramirez, M., 2023. Temporal analysis of the planform morphology of the Quevedo River, Ecuador, using remote sensing. J. South Am. Earth Sci. 128 https://doi.org/10.1016/j. isames.2023.104467.
- Constantine, J.A., Dunne, T., Ahmed, J., Legleiter, C., Lazarus, E.D., 2014. Sediment supply as a driver of river meandering and floodplain evolution in the Amazon Basin. Nat. Geosci. 7 (12), 899–903. https://doi.org/10.1038/ngeo2282.
- Curry, B.B., Grimley, D.A., McKay III, E.D., 2011. Quaternary glaciations in Illinois. In: Ehlers, J., Gibbard, P.L., Hughes, P.D. (Eds.), Developments in Quaternary Science, 15. Elsevier, Amsterdam, The Netherlands, pp. 467–487.
- Dalton, A.S., Margold, M., Stokes, C.R., Tarasov, L., Dyke, A.S., Adams, R.S., Allard, S., Arends, H.E., Atkinson, N., Attig, J.W., Barnett, P.J., Barnett, R.L., Batterson, M., Bernatchez, P., Borns, H.W., Breckenridge, A., Briner, J.P., Brouard, E., Campbell, J. E., Carlson, A.E., Clague, J.J., Curry, B.B., Daigneault, R.A., Dubé-Loubert, H., Easterbrook, D.J., Franzi, D.A., Friedrich, H.G., Funder, S., Gauthier, M.S., Gowan, A.S., Harris, K.L., Hétu, B., Hooyer, T.S., Jennings, C.E., Johnson, M.D., Kehew, A.E., Kelley, S.E., Kerr, D., King, E.L., Kjeldsen, K.K., Knaeble, A.R., Lajeunesse, P., Lakeman, T.R., Lamothe, M., Larson, P., Lavoie, M., Loope, H.M., Lowell, T.V., Lusardi, B.A., Manz, L., McMartin, I., Nixon, F.C., Occhietti, S., Parkhill, M.A., Piper, D.J.W., Pronk, A.G., Richard, P.J.H., Ridge, J.C., Ross, M., Roy, M., Seaman, A., Shaw, J., Stea, R.R., Teller, J.T., Thompson, W.B., Thorleifson, L.H., Utting, D.J., Veillette, J.J., Ward, B.C., Weddle, T.K., Wright, H.E., 2020. An updated radiocarbon-based ice margin chronology for the last deglaciation of the North American Ice Sheet Complex. Quat. Sci. Rev. 234 https://doi.org/10.1016/j.quascirev.2020.106223.
- Daniels, M.D., Rhoads, B.L., 2003. Influence of a large woody debris obstruction on three-dimensional flow structure in a meander bend. Geomorphology 51 (1-3), 159–173. https://doi.org/10.1016/s0169-555x(02)00334-3.
- Daniels, M.D., Rhoads, B.L., 2004. Effect of large woody debris configuration on three-dimensional flow structure in two low-energy meander bends at varying stages. Water Resour. Res. 40 (11) https://doi.org/10.1029/2004wr003181.
- Dawson, M., Lewin, J., 2023. The heterogeneous geomorphological impact of an exceptional flood event and the role of floodplain vegetation. Earth Surf. Process. Landf. https://doi.org/10.1002/esp.5707.
- Donovan, M., Belmont, P., 2019. Timescale dependence in river channel migration measurements. Earth Surf. Process. Landf. 44 (8), 1530–1541. https://doi.org/ 10.1002/esp.4590.
- Donovan, M., Belmont, P., Notebaert, B., Coombs, T., Larson, P., Souffront, M., 2019. Accounting for uncertainty in remotely-sensed measurements of river planform change. Earth-Sci. Rev. 193, 220–236. https://doi.org/10.1016/j.earscirev.2019.04.009.
- Donovan, M., Belmont, P., Sylvester, Z., 2021. Evaluating the relationship between meander-bend curvature, sediment supply, and migration rates. J. Geophys. Res. -Earth Surf. 126 (3) https://doi.org/10.1029/2020jf006058.
- Downward, S.R., Gurnell, A.M., Brookes, A., 1994. A Methodology for Quantifying River Channel Planform Change Using GIS. International Symposium on Variability in Stream Erosion and Sediment Transport,, Canberra, Australia, pp. 449–456.
- Dudley, S.J., Fischenich, J.C., Abt, S.R., 1998. Effect of woody debris entrapment on flow resistance. J. Am. Water Resour. Assoc. 34 (5), 1189–1197. https://doi.org/ 10.1111/j.1752-1688.1998.tb04164.x.
- Faulkner, D.J., 1998. Spatially variable historical alluviation and channel incision in west-central Wisconsin. Ann. Assoc. Am. Geogr. 88 (4), 666–685. https://doi.org/ 10.1111/0004-5608.00117.
- Fehrenbacher, J.B., Olsen, K.R., Jansen, I.J., 1986. Loess thickness in Illinois. Soil Sci. 141, 423–431.
- Ghinassi, M., Moody, J., Martin, D., 2019. Influence of extreme and annual floods on point-bar sedimentation: Inferences from Powder River, Montana, USA. Geol. Soc. Am. Bull. 131 (1-2), 71–83. https://doi.org/10.1130/b31990.1.
- Grimley, D.A., Anders, A.M., Stumpf, A.J., 2016. Quaternary geology of the Upper Sangamon River Basin: Glacial, postglacial, and postsettlement history. In: Lasemi, Z., Elrick, S.D. (Eds.), 1967–2016—Celebrating 50 Years of Geoscience in the Mid-Continent: Guidebook for the 50th Annual Meeting of the Geological Society of America–North-Central Section: Guidebook 43. Illinois State Geological Survey, Champaign, IL, pp. 55–96.
- Grimley, D.A., Anders, A.M., Bettis, E.A., Bates, B.L., Wang, J.J., Butler, S.K., Huot, S., 2017. Using magnetic fly ash to identify post-settlement alluvium and its record of atmospheric pollution, central USA. Anthropocene 17, 84–98. https://doi.org/ 10.1016/j.ancene.2017.02.001.
- Güneralp, I., Rhoads, B.L., 2009. Planform change and stream power in the Kishwaukee River watershed, Illinois: Geomorphic assessment for environmental management. In: James, L.A., Rathburn, S.L., Whittecar, R. (Eds.), Management and Restoration of Fluvial Systems with Broad Historical Changes and Human Impacts. Geological Society of America Special Paper 451, Denver, CO, pp. 109–118.
- Hallberg, G.R., Bettis III, E.A., Prior, J.C., 1984. Geologic overview of the Paleozoic Plateau region of northeastern Iowa. Proc. Iowa Acad. Sci. 91 (1), 5–11.
- Happ, S.C., 1944. Effects of sedimentation on floods in the Kickapoo Valley, Wisconsin. J. Geol. 52, 53–68.
- Hooke, J.M., 1980. Magnitude and distribution of rates of river bank erosion. Earth Surf. Process. Landf. 5 (2), 143–157. https://doi.org/10.1002/esp.3760050205.

- Hooke, J.M., 1987. Lateral migration rates of river bends discussion. J. Hydraul. Eng. -Asce 113 (7), 915–918. https://doi.org/10.1061/(asce)0733-9429(1987)113:7
- Hooke, J.M., 2022. Morphodynamics of a meandering channel over decadal timescales in response to hydrological variations. Earth Surf. Process. Landf. 47 (8), 1902–1920. https://doi.org/10.1002/esp.5354.
- Hooke, J.M., 2023. Morphodynamics of active meandering rivers reviewed in a hierarchy of spatial and temporal scales. Geomorphology 439. https://doi.org/10.1016/j. geomorph.2023.108825.
- Hooke, J.M., Yorke, L., 2011. Channel bar dynamics on multi-decadal timescales in an active meandering river. Earth Surf. Process. Landf. 36 (14), 1910–1928. https://doi. org/10.1002/esp.2214
- Hughes, M.L., McDowell, P.F., Marcus, W.A., 2006. Accuracy assessment of georectified aerial photographs: Implications for measuring lateral channel movement in a GIS. Geomorphology 74 (1-4), 1–16. https://doi.org/10.1016/j.geomorph.2005.07.001.
- Illinois Department of Natural Resources, 1999. Upper Sangamon River Area Assessment: Volume 3 Living Resources. Illinois Natural History Survey, Champaign, IL.
- Illinois Natural Areas Inventory, 2023. INAI Sites By County. Illinois Natural Heritage Database., Available online at https://naturalheritage.illinois.gov/conten t/dam/soi/en/web/naturalheritage/dataresearch/documents/INAICountyList % 20may2023.pdf).
- James, L.A., Lecce, S.A., 2013. Impacts of land-use and land-cover change on river systems. In: J.C. Shroder, Vol. 9, Fluvial Geomorphology, Wohl, E. (Ed). (Ed.), Treatise on Geomorphology. Academic Press, San Diego, CA, pp. 768–793.
- Kasvi, E., Vaaja, M., Alho, P., Hyyppä, H., Hyyppä, J., Kaartinen, H., Kukko, A., 2013. Morphological changes on meander point bars associated with flow structure at different discharges. Earth Surf. Process. Landf. 38 (6), 577–590. https://doi.org/ 10.1002/esp.3303.
- Kelly, S.A., Takbiri, Z., Belmont, P., Foufoula-Georgiou, E., 2017. Human amplified changes in precipitation-runoff patterns in large river basins of the Midwestern United States. Hydrology and Earth System Sciences 21 (10), 5065–5088. https:// doi.org/10.5194/hess-21-5065-2017.
- Kempton, J.P., Johnson, W.H., Heigold, P.C., Cartwright, K., 1991. Mahomet Bedrock Valley in east-central Illinois; topography, glacial drift stratigraphy, and hydrogeology. In: Melhorn, W.N., Kempton, J.P. (Eds.), Geology and Hydrogeology of the Teays-mahomet Bedrock Valley System, GSA Special Paper 258. Geological Society of America, Boulder, CO, pp. 91–129.
- Kessler, A.C., Gupta, S.C., Brown, M.K., 2013. Assessment of river bank erosion in Southern Minnesota rivers post European settlement. Geomorphology 201, 312–322. https://doi.org/10.1016/j.geomorph.2013.07.006.
- Knox, J.C., 1977. Human impacts on Wisconsin stream channels. Ann. Assoc. Am. Geogr. 67 (3), 323–342. https://doi.org/10.1111/j.1467-8306.1977.tb01145.x.
- Knox, J.C., 1987. Historical valley floor sedimentation in the upper Mississippi Valley. Ann. Assoc. Am. Geogr. 77 (2), 224–244. https://doi.org/10.1111/j.1467-8306.1987.tb00155.x.
- Knox, J.C., 2001. Agricultural influence on landscape sensitivity in the Upper Mississippi River Valley. Catena 42 (2-4), 193–224. https://doi.org/10.1016/s0341-8162(00) 00138.7
- Knox, J.C., 2006. Floodplain sedimentation in the Upper Mississippi Valley: Natural versus human accelerated. Geomorphology 79 (3-4), 286–310. https://doi.org/ 10.1016/j.geomorph.2006.06.031.
- Konsoer, K.M., Rhoads, B.L., Langendoen, E.J., Best, J.L., Ursic, M.E., Abad, J.D., Garcia, M.H., 2016. Spatial variability in bank resistance to erosion on a large meandering, mixed bedrock-alluvial river. Geomorphology 252, 80–97. https://doi. org/10.1016/j.geomorph.2015.08.002.
 Kumar, P., Le, P.V.V., Papanicolaou, A.N.T., Rhoads, B.L., Anders, A.M., Stumpf, A.,
- Kumar, P., Le, P.V.V., Papanicolaou, A.N.T., Rhoads, B.L., Anders, A.M., Stumpf, A., Wilson, C.G., Bettis III, E.A., Blair, N., Ward, A.S., Filley, T., Lin, H., Keefer, L., Keefer, D.A., Lin, Y.-F., Muste, M., Royer, T.V., Foufoula-Georgiou, E., Belmont, P., 2018. Critical transition in critical zone of intensively managed landscapes. Anthropocene 22, 10–19. https://doi.org/10.1016/j.ancene.2018.04.002.
- Kumar, P., Anders, A., Bauer, E., Blair, N.E., Cain, M., Dere, A., Druhan, J., Filley, T., Giannopoulos, C., Goodwell, A., Grimley, D., Karwan, D., Keefer, L., Kim, J., Marini, L., Muste, M., Papanicolaou, T., Rhoads, B.L., Rodriguez, L.C.H., Roque-Malo, S., Shafer, S., Stumpf, A., Ward, A., Welp, L., Wilson, C.C., Yan, Q., Zhou, S., 2023. Emergent role of critical interfaces in the dynamics of intensively managed landscapes. Earth-Sci. Rev. 244, 104543 https://doi.org/10.1016/j.earscirev.2023.104543.
- Langhorst, T., Pavelsky, T., 2023. Global observations of riverbank erosion and accretion from Landsat imagery. J. Geophys. Res. -Earth Surf. 128 (2) https://doi.org/ 10.1029/2022jf006774.
- Larsen, E.W., Fremier, A.K., Greco, S.E., 2006. Cumulative effective stream power and bank erosion on the Sacramento River, California, USA. J. Am. Water Resour. Assoc. 42 (4), 1077–1097. https://doi.org/10.1111/j.1752-1688.2006.tb04515.x.
- Lea, D.M., Legleiter, C.J., 2016. Refining measurements of lateral channel movement from image time series by quantifying spatial variations in registration error. Geomorphology 258, 11–20. https://doi.org/10.1016/j.geomorph.2016.01.009.
- Lecce, S.A., 1997. Spatial patterns of historical overbank sedimentation and floodplain evolution: Blue River, Wisconsin. Geomorphology 18 (3-4), 265–277. https://doi. org/10.1016/s0169-555x(96)00030-x.
- Lindroth, E.M., Rhoads, B.L., Castillo, C.R., Czuba, J.A., Guneralp, I., Edmonds, D., 2020. Spatial variability in bankfull stage and bank elevations of lowland meandering rivers: relation to rating curves and channel planform characteristics. Water Resour. Res. 56 (8) https://doi.org/10.1029/2020wr027477.
- Liu, C., Liu, A., He, Y., Chen, Y.H., 2021. Migration rate of river bends estimated by tree ring analysis for a meandering river in the source region of the Yellow River. Int. J. Sediment Res. 36 (5), 593–601. https://doi.org/10.1016/j.ijsrc.2021.04.001.

Magilligan, F.J., 1985. Historical floodplain sedimentation in the Galena River Basin, Wisconsin and Illinois. Ann. Assoc. Am. Geogr. 75 (4), 583–594. https://doi.org/ 10.1111/j.1467-8306.1985.tb00095.x.

- Magilligan, F.J., 1992. Sedimentology of a fine-grained aggrading floodplain.

 Geomorphology 4 (6), 393–408. https://doi.org/10.1016/0169-555x(92)90034-l.
- Mason, J., Mohrig, D., 2019. Scroll bars are inner bank levees along meandering river bends. Earth Surf. Process. Landf. 44 (13), 2649–2659. https://doi.org/10.1002/esp.4600
- Micheli, E.R., Kirchner, J.W., Larsen, E.W., 2004. Quantifying the effect of riparian forest versus agricultural vegetation on river meander migration rates, Central Sacramento River, California, USA. River Res. Appl. 20 (5), 537–548. https://doi.org/10.1002/ prz 756
- Moody, J.A., 2022. The effects of discharge and bank orientation on the annual riverbank erosion along Powder River in Montana, USA. Geomorphology 403. https://doi.org/10.1016/j.geomorph.2022.108134.
- Morais, E.S., Rocha, P.C., Hooke, J., 2016. Spatiotemporal variations in channel changes caused by cumulative factors in a meandering river: the lower Peixe River, Brazil. Geomorphology 273, 348–360. https://doi.org/10.1016/j.geomorph.2016.07.026.
- Nanson, G.C., Hickin, E.J., 1983. Channel migration and incision on the Beatton River. J. Hydraul. Eng., ASCE 109 (3), 327–337. https://doi.org/10.1061/(asce)0733-9429 (1983)109:3(327).
- Nanson, G.C., Hickin, E.J., 1986. A statistical analysis of bank erosion and channel migration in western Canada. Geol. Soc. Am. Bull. 97 (4), 497–504. https://doi.org/ 10.1130/0016-7606(1986)97<497:asaobe>2.0.co;2.
- Neal, C.W.M., Anders, A.M., 2015. Suspended sediment supply dominated by bank erosion in a low-gradient agricultural watershed, Wildcat Slough, Fisher, Illinois, United States. J. Soil Water Conserv. 70 (3), 145–155. https://doi.org/10.2489/ jswc.70.3.145.
- Page, K., Nanson, G., 1982. Concave-bank benches and associated floodplain formation. Earth Surf. Process. Landf. 7 (6), 529–543. https://doi.org/10.1002/ esp. 3290070603
- Pigati, J.S., Rech, J.A., Nekola, J.C., 2010. Radiocarbon dating of small terrestrial gastropod shells in North America. Quat. Geochronol. 5 (5), 519–532. https://doi. org/10.1016/j.quageo.2010.01.001.
- Polvi, L.E., Wohl, E., Merritt, D.M., 2014. Modeling the functional influence of vegetation type on streambank cohesion. Earth Surf. Process. Landf. 39 (9), 1245–1258. https://doi.org/10.1002/esp.3577.
- Quik, C., Wallinga, J., 2018. Reconstructing lateral migration rates in meandering systems - a novel Bayesian approach combining optically stimulated luminescence (OSL) dating and historical maps. Earth Surf. Dyn. 6 (3), 705–721. https://doi.org/ 10.5194/esurf.6-705-2018.
- Quik, C., Candel, J.H.J., Makaske, B., van Beek, R., Paulissen, M., Maas, G.J., Verplak, M., Spek, T., Wallinga, J., 2020. Anthropogenic drivers for exceptionally large meander formation during the Late Holocene. Anthropocene 32. https://doi. org/10.1016/j.ancene.2020.100263.
- Rakovan, M.T., Rech, J.A., Pigati, J.S., Nekola, J.C., Wiles, G.C., 2013. An evaluation of *Mesodon* and other larger terrestrial gastropod shells for dating late Holocene and historic alluvium in the Midwestern USA. Geomorphology 193, 47–56. https://doi.org/10.1016/j.geomorph.2013.03.031.
- Rech, J.A., Tenison, C.N., Baldasare, A., Currie, B.S., 2023. Radiocarbon dating and freshwater reservoir effects of aquatic mollusks within fluvial channel deposits in the midwestern United States. Radiocarbon 65, 1098–1117. https://doi.org/10.1017/ RDC 2023 93
- Rhoads, B.L., 2020. River Dynamics: Geomorphology to Support Management. Cambridge University Press, Cambridge, UK.
- Rhoads, B.L., Herricks, E.E., 1996. Naturalization of headwater streams in Illinois: challenges and possibilities. In: Shields Jr., F.D., Brookes, A. (Eds.), River Channel Restoration. Wiley, Chichester, UK, pp. 331–367.
- Rhoads, B.L., Lewis, Q.W., Andresen, W., 2016. Historical changes in channel network extent and channel planform in an intensively managed landscape: natural versus human-induced effects. Geomorphology 252, 17–31. https://doi.org/10.1016/j. geomorph.2015.04.021.
- Richie, H., 2019. Half of the world's habitable land is used for agriculture. Our World in Data accessed 10/02/2023. (https://ourworldindata.org/global-land-for-agri
- Rodnight, H., Duller, G.A.T., Tooth, S., Wintle, A.G., 2005. Optical dating of a scroll-bar sequence on the Klip River, South Africa, to derive the lateral migration rate of a meander bend. Holocene 15 (6), 802–811. https://doi.org/10.1191/
- Rood, S.B., Bigelow, S.G., Polzin, M.L., Gill, K.M., Coburn, C.A., 2015. Biological bank protection: trees are more effective than grasses at resisting erosion from major river floods. Ecohydrology 8 (5), 772–779. https://doi.org/10.1002/eco.1544.
- Rovey II, C.W., McLouth, T., 2015. A near synthesis of pre-Illinoian till stratigraphy in the central United States: Iowa, Nebraska and Missouri. Quat. Sci. Rev. 126, 96–111. Rowland, J., Schwenk, J., 2019. Global meta-analysis of published river bank erosion and migration rates. Ess. -Dive.
- Salas, C.R., Rhoads, B.L., 2022. Big Pine Creek Ditch revisited: Planform recovery to channelization and the timescale of river meandering. Geomorphology 403. https:// doi.org/10.1016/j.geomorph.2022.108140.
- Schook, D.M., Rathburn, S.L., Friedman, J.M., Wolf, J.M., 2017. A 184-year record of river meander migration from tree rings, aerial imagery, and cross sections. Geomorphology 293, 227–239. https://doi.org/10.1016/j.geomorph.2017.06.001.
- Soller, D.R., Price, S.D., Kempton, J.P., Berg, R.C., 1999. Three-Dimensional Geologic Maps of Quaternary Sediments in East-Central. Illinois. U.S. Geological Survey, Geologic Investigations Series Map I-2669,, 1:500,000.

Stuiver, M., Polach, H.A., 1977. Reporting of C-14 data- discussion. Radiocarbon 19 (3), 355–363. https://doi.org/10.1017/s0033822200003672.

B.L. Rhoads et al.

- Stuiver, M., Reimer, P.J., 1993. Extended C-14 data base and revised Calib 3.0C-14 age calibration program. Radiocarbon 35 (1), 215–230. https://doi.org/10.1017/ s0033822200013904.
- Stumpf, A.J., Dey, W.S., 2012. Understanding the Mahomet Aquifer: Geological, Geophysical, and Hydrogeological Studies in Champaign County and Adjacent Areas. Ilinois State Geological Survey, draft report to Illinois American Water,, Champaign, IL contract no. 2007-02899. Available online at. https://hdl.handle.net/2142/95787).
- Sylvester, Z., Durkin, P.R., Hubbard, S.M., Mohrig, D., 2021. Autogenic translation and counter point bar deposition in meandering rivers. Geol. Soc. Am. Bull. 133 (11-12), 2439–2456. https://doi.org/10.1130/b35829.1.
- Trimble, S.W., 1983. A sediment budget for Coon Creek Basin in the Driftless Area, Wisconsin, 1853-1977. Am. J. Sci. 283 (5), 454–474.
- Trimble, S.W., 2009. Fluvial processes, morphology and sediment budgets in the Coon Creek Basin, WI, USA, 1975-1993. Geomorphology 108 (1-2), 8–23. https://doi.org/10.1016/j.geomorph.2006.11.015.
- Trimble, S.W., 2013. Historical Agriculture and Soil Erosion in the Upper Mississippi River Hill Country. CRC Press, Boca Raton, Florida.
- Urban, M.A., Rhoads, B.L., 2003. Catastrophic human-induced change in stream-channel planform and geometry in an agricultural watershed, Illinois, USA. Ann. Assoc. Am. Geogr. 93 (4), 783–796. https://doi.org/10.1111/j.1467-8306.2003.09304001.x.
- White, A.B., Kumar, P., Saco, P.M., Rhoads, B.L., Yen, B.C., 2003. Changes in hydrologic response due to stream network extension via land drainage activities. Journal of the

- American Water Resources Association 39 (6), 1547–1560. https://doi.org/10.1111/j.1752-1688.2003.tb04438.x.
- Wilson, C.G., Abban, B., Keefer, L.L., Wacha, K., Dermisis, D., Giannopoulos, C., Zhou, S. N., Goodwell, A.E., Woo, D.K., Yan, Q.N., Ghadiri, M., Stumpf, A., Pitcel, M., Lin, Y. F., Marini, L., Storsved, B., Goff, K., Vogelgsang, J., Dere, A., Schilling, K.E., Muste, M., Blair, N.E., Rhoads, B., Bettis, A., Pai, H., Kratt, C., Sladek, C., Wing, M., Selker, J., Tyler, S., Lin, H., Kumar, P., Papanicolaou, A.N., 2018. The intensively managed landscape critical zone observatory: a scientific testbed for understanding critical zone processes in agroecosystems. Vadose Zone J. 17 (1) https://doi.org/10.2136/vzj2018.04.0088.
- Yu, G.A., Li, Z.W., Yang, H.Y., Lu, J.Y., Huang, H.Q., Yi, Y.J., 2020. Effects of riparian plant roots on the unconsolidated bank stability of meandering channels in the Tarim River, China. Geomorphology 351. https://doi.org/10.1016/j. geomorph.2019.106958.
- Yu, M., 2018. Analysis of Sediment Dynamics in Intensively Manage Landscapes.

 Doctoral Dissertation. University of Illinois, Urbana, IL (Available at). (https://www.ideals.illinois.edu/items/109815).
- Yu, M., Rhoads, B.L., 2018. Floodplains as a source of fine sediment in grazed landscapes: Tracing the source of suspended sediment in the headwaters of an intensively managed agricultural landscape. Geomorphology 308, 278–292. https://doi.org/ 10.1016/j.geomorph.2018.01.022.
- Zhu, L.K., Chen, D., Hassan, M.A., Venditti, J.G., 2022. The influence of riparian vegetation on the sinuosity and lateral stability of meandering channels. Geophys. Res. Lett. 49 (2) https://doi.org/10.1029/2021gl096346.